Patch near-field acoustic holography: Regularized extension and statistically optimized methods

Jean-Claude Pascal,[a] Sébastien Paillasseur, and Jean-Hugh Thomas
Laboratoire d'Acoustique de l'Université du Maine (CNRS UMR 6613) and Ecole Nationale Supérieure d'Ingénieurs du Mans (ENSIM), Université du Maine, rue Aristote, 72000 Le Mans, France

Jing-Fang Li
Visual VibroAcoustics, 51 rue d'Alger, 72000 Le Mans, France

(Received 29 September 2008; revised 10 June 2009; accepted 7 July 2009)

The patch holography method allows one to make measurements on an extended structure using a small microphone array. Increased attention has been paid to the two techniques, which are quite different at first glance. One is to extrapolate the pressure field measured on the hologram plane while the other is to use statistically optimized processing. A singular value decomposition formulation of the latter is proposed in this paper. The similarity of the two techniques is shown here. Both use a convolution of the measured pressure patch to obtain a better estimate of the wavenumber spectrum backward propagated on the structure. By using the Morozov discrepancy principle to compute the regularization parameter, the two methods lead to very close results.
 [DOI: 10.1121/1.3192349]

PACS number(s): 43.60.Sx, 43.60.Pt, 43.20.Ye, 43.40.Sk [EGW] Pages: 1264–1268

I. INTRODUCTION

A fundamental assumption of planar near-field acoustic holography (NAH) is that the measurement plane in the near-field of sources is infinite. In practice it is enough that the measurement plane is significantly larger than the radiating surface so that the field reconstruction can be done under good conditions. As soon as the dimensions of the hologram decrease, the truncation effect of the measured field creates distortions mainly due to the use of the discrete spatial Fourier transform (DSFT). These distortions can be reduced by using a Tukey window[1] but with the impossibility to use the whole reconstructed field, by selectively filtering the edge effects using wavelets,[2] or by regularizing an inversion technique of the transfer matrix representing the propagation,[3,4] eventually associated with a condensation method.[5,6] The analysis of an extended emitting area with a small microphone array is often found in applications of acoustic holography, and the fundamental assumption is rarely satisfied. To overcome this important limitation, methods known as "patch holography" have been proposed.[7–11] When the array (patch) is smaller than the radiating area, for example, in case of a large vibrating structure, these techniques allow one to reconstruct the field on the projected area from the hologram with a minimum of distortion caused by the edge effects and the sound field emitted by the surfaces not covered by the array.

Essentially two methods are used to solve this problem: (i) a method by which the field on the hologram is extrapolated over a larger area by using an iterative process,[7–9,12–14] and (ii) a method that uses statistical optimization for estimating the wavenumber spectrum from an acquisition on a small aperture hologram.[10,11,15–17]

The first method was introduced by Saijyou and Yoshikawa.[7] They showed that a sound field measured over the patch can be extended into the exterior region by using an iterative data restoration algorithm that increases the aperture size by limiting the bandwidth of the wavenumber spectrum. This method has been further optimized by Williams *et al.*[8,9] by using a modified Tikhonov filter with a regularization technique, and the discrete Fourier transform formulation has also been extended in terms of singular value decomposition (SVD). Since this technique was implemented for cylindrical geometries[12] and applied to recovery a source distribution from hologram pressures was measured over multiple unconnected patches.[14] Variants for performing patch NAH were also proposed: a one-step procedure using Tikhonov regularization with generalized cross validation[13] and methods using a sound field model in terms of spherical harmonics[18] or equivalent sources.[5,6]

The second technique introduced by Steiner and Hald[10] optimizes the NAH process by realizing a spatial convolution to have a wavenumber spectrum produced by only the source region covered by the patch. The spatial convolution is obtained by imposing constraints on the wavenumber spectrum. This method has been adapted to different experimental configurations[11,16,17] and cylindrical geometries.[15]

The scope of this paper is to compare the two methods. So the processing algorithms are formulated with the same notations, then the performances of the two methods are illustrated by a simple example.

II. SOME NAH PROBLEMS

Consider a planar surface Γ_s corresponding to the source area on which the pressure and normal velocity fields are,

[a]Author to whom correspondence should be addressed. Electronic mail: jean-claude.pascal@univ-lemans.fr

respectively, $p(\mathbf{y})$ and $u_z(\mathbf{y})$. Another surface Ω is located at a small distance d in the near-field, on which the acoustic pressure $p(\mathbf{x})$ is measured. The discrete space Fourier transform of the Helmholtz equation allows one to write as

$$\mathbf{p}(\mathbf{x}) = \mathbf{W}\mathbf{P}(\mathbf{k}) = \begin{cases} \mathbf{W}\mathbf{G}_N\mathbf{W}^+\mathbf{u}(\mathbf{y}) \\ \mathbf{W}\mathbf{G}_D\mathbf{W}^+\mathbf{p}(\mathbf{y}), \end{cases} \quad (1)$$

where $\mathbf{p}(\mathbf{x})$ is the column vector of M elements of the measured pressure on the mesh of a finite surface Ω, and $\mathbf{u}(\mathbf{y})$ and $\mathbf{p}(\mathbf{y})$ are, respectively, the vectors of velocity and pressure on Γ_s. $\mathbf{W}$ is the matrix of the backward Fourier transform that allows one to obtain the vector of pressure $\mathbf{p}(\mathbf{x})$ from its discrete wavenumber spectrum denoted by the vector $\mathbf{P}(\mathbf{k})$. The elements of the matrix $\mathbf{W}$ are written by $W_{mn} = \exp(-j\mathbf{k}_n \cdot \mathbf{x}_m)/\sqrt{M}$. The forward Fourier transform is defined here as the generalized inverse $\mathbf{W}^+$ of the backward Fourier transform, such that $\mathbf{W}\mathbf{W}^+ = \mathbf{I}$. This definition allows one to obtain an estimate of wavenumber spectrum from an irregular sampling of the hologram,[19] as it is done for the statistically optimal near-field acoustic holography (SONAH) method.[11] In this case, the matrix of the backward transform used for the inverse of matrix corresponds to an overdetermined system, which leads to the estimate of the wavenumber spectrum in the least square sense. In the particular case of a regular grid and a square matrix (as used in the examples of Sec. IV), the authors have the equivalent equation $\mathbf{W}^+ \equiv \mathbf{W}^H$. In practice, the matrix $\mathbf{W}$ used to recover the field from the wavenumber spectrum is often different from that which is used to calculate the forward Fourier transform. In fact, independently of the measurement mesh, the field is presented on a regular grid of which the number of points is strongly increased to visually get a better resolution. $\mathbf{W}$ is a rectangular matrix with the number of rows (points of the field) being much more significant than the number of columns (points of the wavenumber spectrum). This operation corresponds to a Shannon interpolation and no more information is added. This method gets the same results as the iterative procedure proposed in Ref. 14, while being much faster.

The diagonal matrices $\mathbf{G}_N$ and $\mathbf{G}_D$ are the propagators, the elements of which are expressed as $G_{N,n} = -\rho c k e^{-jk_z d}/k_z$ and $G_{D,n} = e^{-jk_z d}$, respectively, with $k_z = \sqrt{k^2 - \mathbf{k}_n^2}$ ($k = \omega/c$ and $\sqrt{-1} = -j$). The inversion of Eq. (1) allows one to reconstruct with a good accuracy, the pressure $\mathbf{p}(\mathbf{y})$ and the velocity $\mathbf{u}(\mathbf{y})$ from the measured pressure $\mathbf{p}(\mathbf{x})$ provided that the hologram is larger than the source region and that the evanescent waves amplified by the inverse propagator are filtered by a low-pass filter represented by the diagonal matrix $\mathbf{F}_\alpha = \mathrm{diag}(F_\alpha)$ as follows:[20,21]

$$\tilde{\mathbf{u}}(\mathbf{y}) = \mathbf{W}\mathbf{G}_N^{-1}\mathbf{F}_\alpha\mathbf{W}^+\mathbf{p}(\mathbf{x}), \quad (2)$$

$$\tilde{\mathbf{p}}(\mathbf{y}) = \mathbf{W}\mathbf{G}_D^{-1}\mathbf{F}_\alpha\mathbf{W}^+\mathbf{p}(\mathbf{x}). \quad (3)$$

The reconstruction of $\tilde{\mathbf{u}}(\mathbf{y})$ and $\tilde{\mathbf{p}}(\mathbf{y})$ is thus smoothed by the removal of the components whose spatial oscillations have short wavelengths. Williams *et al.*[1,9] described in detail the consequences of the discretization in the spatial and wavenumber domains and the role of the spatial periodicity

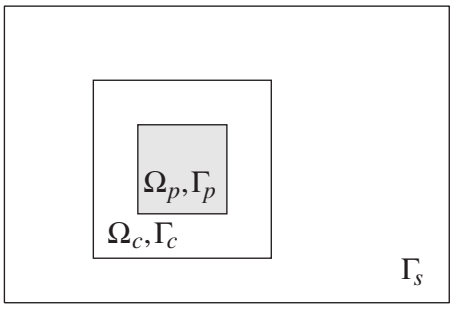

FIG. 1. Ω_p, pressure measurement surface (patch); Ω_c, band around the patch; Γ_p and Γ_c, corresponding to normal projection area on source surface; and Γ_s, whole radiating surface.

of the pressure $\mathbf{p}(\mathbf{x})$ on adjacent regions to Ω (aperture replication problem). The operation of reconstruction of the velocity on Γ_s is a convolution of this periodic pressure field, which causes an expansion and a recovering of the border areas on adjacent regions. The authors now consider that the measurement surface Ω is reduced to a patch Ω_p. This patch is smaller than the source area Γ_s (see Fig. 1). Γ_p is the normal projection of the patch on the source plane where the pressure and velocity fields are to be reconstructed. The reduction in the hologram size makes the problem of spatial periodicity more critical. The technique of zero-padding has long been used as a solution[1] for the effect of convolution mentioned above. It does not, however, allow one to reduce the influence of the part of Γ_s outside Γ_p or the edge discontinuity effects.

III. PATCH NAH METHODS

The objective is, in the case of an extended source region Γ_s, to reconstruct as accurately as possible the field on Γ_p from the pressure measurements on Ω_p (see Fig. 1).

A. Iterative method for extension of the hologram

The iteration method for extension of the hologram was proposed by Saijyou and Yoshikawa[7] and then improved by Williams *et al.*[8,9] who also showed that DSFT and SVD approaches provide comparable results. It is the DSFT approach that is used here. The method is to extrapolate the pressure $\mathbf{p}(\mathbf{x} \in \Omega_p)$ over the domain Ω_c. Initially the band Ω_c is filled with zeros. The zero-padding technique is implemented using a $M_1 \times M$ rectangular matrix $\mathbf{R}$ with elements equal to 1 or 0 (where $M_1 > M$), such as

$$\mathbf{p}_0(\mathbf{x}) = \mathbf{R}\mathbf{p}(\mathbf{x}) = \begin{cases} \mathbf{p}(\mathbf{x} \in \Omega_p) & \text{(measurements)} \\ 0(\mathbf{x} \in \Omega_c) & \text{(zero-padding)}. \end{cases} \quad (4)$$

The transpose of the matrix $\mathbf{R}$ allows one to extract the pressure on the surface of the patch Ω_p: $\mathbf{p}(\mathbf{x}) = \mathbf{R}^T\mathbf{p}_0(\mathbf{x})$. After zero-padding and filtering, the smoothed pressure

$$\tilde{\mathbf{p}}_0(\mathbf{x}) = \mathbf{W}\mathbf{F}_{N,\alpha}\mathbf{W}^+\mathbf{p}_0(\mathbf{x}) = \mathbf{W}\mathbf{F}_{N,\alpha}\mathbf{W}^+\mathbf{R}\mathbf{p}(\mathbf{x}) \quad (5)$$

is extended on the whole field $\Omega_p \cup \Omega_c$ by the effect of a low-pass filter in the wavenumber domain represented by the diagonal matrix $\mathbf{F}_{N,\alpha}$. To refine the process of extrapolation, several iterations are used as follows:

$$\tilde{\mathbf{p}}_{i+1}(\mathbf{x}) = \mathbf{W}\mathbf{F}_{N,\alpha_i}\mathbf{W}^{+}[(\mathbf{I}-\mathbf{R}\mathbf{R}^{T})\tilde{\mathbf{p}}_i(\mathbf{x}) + \mathbf{R}\mathbf{p}(\mathbf{x})], \tag{6}$$

where $\mathbf{I}-\mathbf{R}\mathbf{R}^T$ is a diagonal matrix that selects the points on the band Ω_c. The iteration procedure starts with $i=0$ and $\tilde{\mathbf{p}}_0(x)$ given by Eq. (5). The process is stopped at $i=I$ when the desired convergence $\|\tilde{\mathbf{p}}_{i+1}-\tilde{\mathbf{p}}_i\| < \varepsilon$ is reached. For each new iteration, the measured pressure field on the patch $\mathbf{p}(\mathbf{x} \in \Omega_p)$ replaces the corresponding part of the smoothed field $\tilde{\mathbf{p}}_i(x)$, without changing the estimate in Ω_c. A fundamental point of the method[8,9] is the use of the modified Tikhonov regularization filter[21]

$$F_{N,\alpha_i}(\mathbf{k}_n) = \lambda_n^2[\lambda_n^2 + \alpha_i(\alpha_i/[\alpha_i + \lambda_n^2])^2]^{-1}, \tag{7}$$

where $\lambda_n^2=|G_N(\mathbf{k}_n)|^2$ for $\mathbf{F}_{N,\alpha}$. This filter contains the information about the propagation process and depends on the distance d separating the Ω_p and Γ_p planes. The parameter α_i is updated at each iteration according to the standard deviation σ_i of the noise, which is estimated in the wavenumber domain with the assumption that beyond a cut-off value $\mathbf{k}^2 > k_c^2$, the spectrum only holds noise

$$\sigma_i \approx \|\mathbf{D}\mathbf{P}_i(\mathbf{k})\|_F/\|\mathbf{D}\|_F, \tag{8}$$

where $\|\cdot\|_F$ is the Frobenius norm, $\mathbf{D}=\mathrm{diag}(D_n)$, with $D_n(\mathbf{k})=1$ when $\mathbf{k}^2 \geq k_c^2$ and $D_n(\mathbf{k})=0$ otherwise. k_c corresponds to the maximum wavenumber in agreement with the sampling criterion.[21] According to Eq. (6), the non-smoothed pressure is $\mathbf{p}_i(\mathbf{x})=(\mathbf{I}-\mathbf{R}\mathbf{R}^T)\tilde{\mathbf{p}}_{i-1}(\mathbf{x})+\mathbf{R}\mathbf{p}(\mathbf{x})$. Once the standard deviation is computed, an automatic selection of the regularization parameter α_i is obtained by verifying the following relation called the Morozov discrepancy principle:

$$\|\tilde{\mathbf{p}}_i(\mathbf{x}) - \mathbf{p}_i(\mathbf{x})\|_F/\sqrt{M_1} = \|(\mathbf{F}_{N,\alpha_i}-\mathbf{I})\mathbf{P}_i(\mathbf{k})\|_F/\sqrt{M_1} \equiv \sigma_i. \tag{9}$$

The regularization parameter depending on the bounds of the exact solution is not known in advance. A classical strategy due to Morozov determines this regularization parameter by solving a non-linear scalar equation,[22] in this case by an iterative computation. Morozov's principle is established when the discrepancy of the corresponding regularized solution is just equal to the measurement error. Williams[21] described the use of this principle to determine the regularization parameter from the estimated noise by considering the wavenumber spectrum outside the circle of radius k_c. In this procedure noise is considered in a general sense; it also includes the distortions due to the truncation of the field and the errors of spatial undersampling (Shannon's criterion is never ensured in NAH). Finally the reconstructed velocity on Γ_p can be written by

$$\tilde{\mathbf{u}}(\mathbf{y}) = \mathbf{R}^T\mathbf{W}\mathbf{G}_N^{-1}\mathbf{W}^{+}\tilde{\mathbf{p}}_I(\mathbf{x}). \tag{10}$$

The filter of Eq. (7) uses the propagator G_N that supposes that the extrapolated field is optimized for reconstructing the velocity by using Eq. (2). To reconstruct the pressure using Eq. (3), it will be necessary to substitute G_D for G_N and $\mathbf{F}_{D,\alpha}$ for $\mathbf{F}_{N,\alpha}$ in the iteration procedure of Eq. (6).

B. Method of the statistically optimized backpropagation

The method of the statistically optimized backpropagation was proposed by Hald and co-worker[10,11] for the plane geometry under the name of SONAH then adapted to cylindrical geometries[15] and to the reconstruction of other quantities.[16,17] In this method, the transfer matrix $\mathbf{H}_D$ used to compute the pressure on the source plane from a small hologram aperture

$$\mathbf{p}(\mathbf{y}) = \mathbf{H}_D\mathbf{p}(\mathbf{x}) \tag{11}$$

is obtained using the approach completely different from that given by Eq. (3). An optimized solution is searched to correct, as well as possible, all the distortions of the reconstruction process such as small size of the patch, discontinuity at the edges, and influence of noise in the restoration of evanescent waves. For this purpose, a set of elementary solutions for which one knows the correspondence on the Ω_p and Γ_p planes is employed. In fact, these elementary solutions are projections of plane waves whose angle of incidence is associated with each point $\mathbf{k}_n$ of the wavenumber spectrum. For example, $\mathbf{H}_D$ should satisfy the following expression:

$$\mathbf{p}_n(\mathbf{y}) = \mathbf{H}_D\mathbf{p}_n(\mathbf{x}), \tag{12}$$

where $\mathbf{p}_n(\mathbf{y})=[e^{-j\mathbf{k}_n\cdot\mathbf{y}}]=\mathbf{R}^T\mathbf{W}\sqrt{M}\ \mathrm{diag}(\delta_{\ell n})$ and $\mathbf{p}_n(\mathbf{x})=[e^{-jk_z d}e^{-j\mathbf{k}_n\cdot\mathbf{x}}]=\mathbf{R}^T\mathbf{W}\mathbf{G}_D\sqrt{M}\ \mathrm{diag}(\delta_{\ell n})$, with $k_z=\sqrt{k^2-\mathbf{k}_n^2}$. $\mathrm{diag}(\delta_{\ell n})$ is a diagonal matrix having only one element equal to 1 (when $\ell=n$, $\delta_{\ell n}=1$) corresponding to the plane wave with wavenumber vector $\mathbf{k}_n$. All other points of the wavenumber spectrum must also satisfy Eq. (12). All these constraints are synthesized in a matrix form by the following equation:

$$[\mathbf{p}_1(\mathbf{y})\cdots\mathbf{p}_n(\mathbf{y})\cdots\mathbf{p}_N(\mathbf{y})] = \mathbf{H}_D[\mathbf{p}_1(\mathbf{x})\cdots\mathbf{p}_n(\mathbf{x})\cdots\mathbf{p}_N(\mathbf{x})],$$

$$\mathbf{R}^T\mathbf{W} = \mathbf{H}_D\mathbf{R}^T\mathbf{W}\mathbf{G}_D. \tag{13}$$

It is the transposed form of Eq. (13) that was used in Ref. 11. By introducing a $M\times N$ rectangular matrix $\mathbf{W}_R=\mathbf{R}^T\mathbf{W}$ (where $N>M$), Eq. (13) can be written as $\mathbf{W}_R=\mathbf{H}_D\mathbf{A}$, where $\mathbf{A}=\mathbf{W}_R\mathbf{G}_D$. The authors can see that the number of points of the wavenumber spectrum is larger than that on the patch. This important issue discussed below leads to a system to which the solution $\mathbf{H}_{D,\alpha}$ is obtained by computing the (regularized) Moore–Penrose generalized right inverse[23] of matrix $\mathbf{A}$,

$$\mathbf{H}_{D,\alpha} = \mathbf{W}_R\mathbf{A}^H(\mathbf{A}\mathbf{A}^H + \alpha\mathbf{I})^{-1}. \tag{14}$$

Substituting Eq. (14) and the expression for $\mathbf{A}$ into Eq. (11) yields

$$\tilde{\mathbf{p}}(\mathbf{y}) = \mathbf{W}_R\mathbf{G}_D^H\mathbf{W}_R^H(\mathbf{W}_R\mathbf{G}_D\mathbf{G}_D^H\mathbf{W}_R^H + \alpha\mathbf{I})^{-1}\mathbf{p}(\mathbf{x}). \tag{15}$$

Each element of the matrix $\mathbf{A}\mathbf{A}^H=\mathbf{W}_R\mathbf{G}_D\mathbf{G}_D^H\mathbf{W}_R^H$ represents the sum of the whole wavenumber spectrum. If $\mathbf{W}_R$ is a square matrix, the operation is an ordinary DSFT on the patch, without optimization. It is the number of points of the K-spectrum higher than the number of points of the hologram ($N>M$), which allows an optimization for the small size of the patch by increasing the number of constraints

imposed on the wavenumber spectrum. By considering that $N \to \infty$, Hald[11] gave analytical expressions for the elements of the matrix $\mathbf{AA}^H$. The regularization factor can be obtained in the same way as for the iterative method, by estimating the standard deviation of the noise using Eq. (8) and by evaluating α by means of the Morozov discrepancy principle.

An alternative formulation of the SONAH method can be obtained by carrying out the SVD of matrix $\mathbf{A}$, such as $\mathbf{A}=\mathbf{U}\ \mathrm{diag}(\lambda_n)\mathbf{V}^H$. Substituting this expression into Eq. (14) results in an expression equivalent to Eq. (15) as follows:

$$\tilde{\mathbf{p}}(\mathbf{y}) = \mathbf{W}_R \mathbf{V} \mathbf{F}_\alpha\ \mathrm{diag}(\lambda_n^{-1}) \mathbf{U}^H \mathbf{p}(\mathbf{x}), \tag{16}$$

where $\mathbf{F}_\alpha$ is the diagonal matrix of a filter whose elements are given by $F_\alpha = \lambda_n^2/(\alpha+\lambda_n^2)$, where λ_n^2 are the eigenvalues of the decomposition of the matrix $\mathbf{A}$. It should be noted that unlike the use of the SVD to compute the inverse of the projection matrix between the hologram and the source plane,[3,13,21] here the inverse is applied only to the model of the transfer matrix between the points of the patch and those of the wavenumber spectrum backpropagated to the Γ_s plane. A statistically optimized solution for the reconstruction of the velocity can be obtained in the same way by substituting G_N for G_D, but because of the bad conditioning introduced by the use of propagator G_N, the choice of the direct calculation of the derivative of Eq. (15) was often made, as was done in Ref. 16.

IV. RESULTS AND DISCUSSION

A. Common expressions for the two techniques

It is noteworthy that from the previous results [Eqs. (10), (15), and (16)], the two methods can be presented in one formulation as follows:

$$\tilde{\mathbf{s}}(\mathbf{y}) = \mathbf{R}^T \mathbf{W} \tilde{\mathbf{S}}(\mathbf{k}) \quad \text{with} \quad \tilde{\mathbf{S}}(\mathbf{k}) = \mathbf{C}_{\eta,\alpha} \mathbf{p}(\mathbf{x}), \tag{17}$$

where $\tilde{\mathbf{s}}(\mathbf{y})$ can be the pressure $\tilde{\mathbf{p}}(\mathbf{y})$ or the velocity $\tilde{\mathbf{u}}(\mathbf{y})$ on the area Γ_p. In all cases, the matrix $\mathbf{C}_{\eta,\alpha}$ represents a convolution of the pressure $\mathbf{p}(\mathbf{x})$ on the patch Ω_p followed by a transformation that allows one to estimate the regularized wavenumber spectrum $\tilde{\mathbf{S}}(\mathbf{k})$ of the velocity or the pressure on Γ_p (η could be D or N according to the propagator). For the method of extension of the patch, the convolution matrix is implicitly defined in recursive form by Eq. (6),

$$\mathbf{C}_{\eta,\alpha} \mathbf{p}(\mathbf{x}) = \mathbf{G}_\eta^{-1} \mathbf{W}^+ \tilde{\mathbf{p}}_I(\mathbf{x}). \tag{18}$$

In the case of the SONAH method, the convolution matrix is defined from Eqs. (15) and (16) as

$$\begin{aligned} \mathbf{C}_{\eta,\alpha} &= \mathbf{G}_\eta^H \mathbf{W}^H \mathbf{R} (\mathbf{R}^T \mathbf{W} \mathbf{G}_\eta \mathbf{G}_\eta^H \mathbf{W}^H \mathbf{R} + \alpha \mathbf{I})^{-1} \\ &= \mathbf{V} \mathbf{F}_\alpha\ \mathrm{diag}(\lambda_n^{-1}) \mathbf{U}^H, \end{aligned} \tag{19}$$

where η is the propagator of the pressure or the velocity adapting to the reconstruction process.

Both methods are clearly the techniques of optimization of the wavenumber spectrum reconstructed on the plane Γ_p, and the following example gives an illustration.

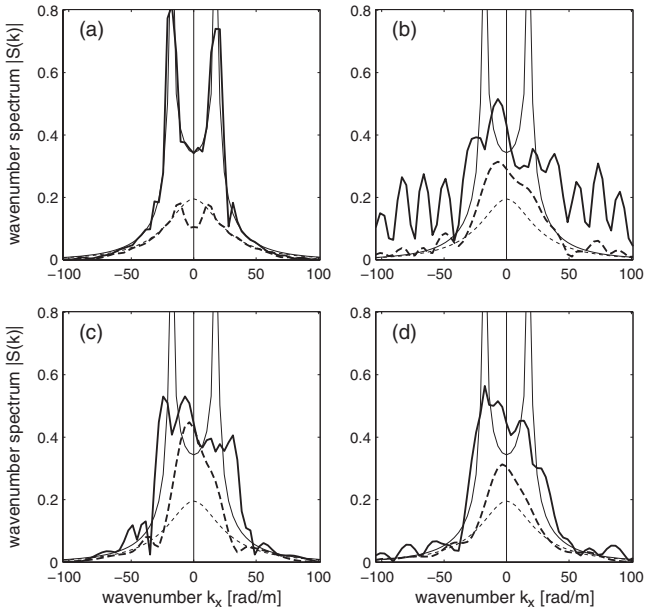

FIG. 2. Computed values (thick lines) and theoretic values obtained by Eq. (20) (thin lines) of cross-section slices of wavenumber spectra backpropagated from $d=3$ cm to the plane Γ_s for a point source located 5 cm from the hologram (1000 Hz, SNR: 40 dB) for $k_y=0$ (solid lines) and $k_y=1.5\ k$ (dashed lines). (a) Hologram of 60×60 grid points, Tukey window at 50%, modified Tikhonov filter and DSFT; (b) patch of 12×12 and zero-padding of 60×60 grid points, modified Tikhonov filter and DSFT; (c) patch of 12×12 and expansion on a 60×60 mesh with modified Tikhonov filter and 800 iterations; and (d) patch of 12×12, SONAH with regularization.

B. Illustration by a simple example

Consider a point source ($f=1000$ Hz) at $(x_0,y_0)=(5\ \mathrm{cm},\ 9\ \mathrm{cm})$ with respect to the origin at the center of the hologram. The hologram plane is at 5 cm from the source. The field is backpropagated 3 cm toward the source (the plane Γ_s is therefore at $z_0=2$ cm from the source center). A white noise with a signal-to-noise ratio (SNR) of 40 dB is added. Two cross-section slices of the wavenumber spectra on the plane Γ_s, versus k_x for $k_y=0$ (solid lines) and $k_y=1.5\ k$ (dashed lines) within the region of evanescent waves, are shown in Figs. 2(a)–2(d). The computed values are shown by thick lines. The theoretical wavenumber spectrum for the unit point source[24] obtained by

$$S(\mathbf{k}) = \frac{-\rho c k e^{-j(k_x x_0 + k_y y_0 + k_z z_0)}}{k_z} \tag{20}$$

is shown in Fig. 2 by thin lines. The reference K-spectrum shown in Fig. 2(a) is computed from 60×60 grid points with a spatial step size of 3 cm. A Tukey window at 50% is applied before Fourier transformation (DSFT), filtering, and backpropagation, according to Eq. (3). Figures 2(b)–2(d) show the results reconstructed from measurements on a patch of 12×12 grid points by the use of different processing that allows a K-spectrum on a 60×60 mesh to be obtained. The results shown in Fig. 2(b) is obtained by simply applying DSFT after zero-padding and filtering: $\mathbf{G}_D^{-1}\mathbf{F}_\alpha\mathbf{W}^+\mathbf{R}\mathbf{p}(\mathbf{x})$. For results shown in Fig. 2(c), the method of extension of the patch is employed [Eq. (18)] with 800 iterations of Eq. (6). To obtain the results shown in Figs. 2(a)–2(c), a modified Tikhonov filter [Eq. (7)] is used with a coefficient of regu-

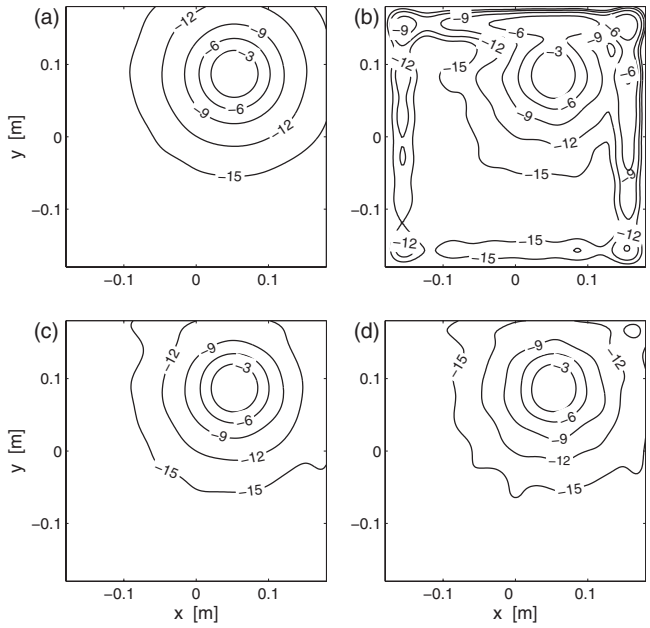

FIG. 3. Reconstruction on Γ_p area (normal projection of the patch) for the four processing methods shown in Fig. 2. Contours of pressure amplitude in decibels.

larization α determined by using Eqs. (8) and (9). Figure 2(d) corresponds to the SONAH method using the SVD formulation, but the two formulas of this method strictly check the equality of Eq. (19). The same number of points (60×60) is used for the wavenumber spectrum in the four configurations. Thus, in all the cases, the matrix $\mathbf{R}$ in Eqs. (6), (17), and (19) is of size $60^2 \times 12^2$. Finally, Fig. 3 shows the pressure on the normal projection Γ_p of the patch, by performing the backward Fourier transform of the K-spectra shown in Fig. 2. The important distortions of K-spectrum in Fig. 2(b) are caused by severe aliasing effects on the projected field [see Fig. 3(b)]. Although the cross-section slice of wavenumber spectra shown in Figs. 2(c) and 2(d) still deviates from the theoretical values or from the curves in Fig. 2(a), the projected fields shown in Figs. 3(c) and 3(d) allow one to obtain the pressure fields without too many distortions.

V. CONCLUSIONS

The same notation is used to express two methods of patch holography: the regularized extension method by iteration process and the statistically optimized method. A fundamental aspect is associated with the rectangular matrix $\mathbf{R}$, which describes the extension of the initial field by zero-padding for the iterative method and of the additional constraints imposed on the wavenumber spectrum by increasing the density of points. For the latter technique, an alternative formulation using the SVD is established. By determining the regularization parameter using the Morozov discrepancy principle, the methods of iterative expansion and SONAH provide similar results with pressure to pressure propagator. The iterative method is more expensive in computing times but seems to be more robust when the SNR decreases. Both make significant improvements to the standard NAH.

[1] E. G. Williams, *Fourier Acoustics* (Academic, London, 1999).
[2] J.-H. Thomas and J.-C. Pascal, "Wavelet preprocessing for lessening truncation effects in nearfield acoustical holography," J. Acoust. Soc. Am. **118**, 851–860 (2005).
[3] P. A. Nelson and S. H. Yoon, "Estimation of acoustic sources strength by inverse methods: Part I, Conditioning of the inverse problem," J. Sound Vib. **233**, 634–668 (2000).
[4] E. G. Williams, "Comparison of SVD and DFT approaches for NAH," Proceedings of the Inter-Noise 2002, Dearborn, MI, 19–21 August (2002).
[5] A. Sarkissian, "Method of superposition applied to patch near-field acoustic holography," J. Acoust. Soc. Am. **118**, 671–678 (2005).
[6] C. Bi, X. Chen, L. Xu, and J. Chen, "Patch nearfield acoustic holography based on the equivalent source method," Sci. China, Ser. E: Technol. Sci. **51**, 100–110 (2008).
[7] K. Saijyou and S. Yoshikawa, "Reduction methods of the reconstruction error for large-scale implementation of near-field acoustical holography," J. Acoust. Soc. Am. **110**, 2007–2023 (2001).
[8] E. G. Williams, "Continuation of acoustic near-fields," J. Acoust. Soc. Am. **113**, 1273–1281 (2003).
[9] E. G. Williams, B. H. Houston, and P. C. Herdic, "Fast Fourier transform and singular value decomposition formulations for patch nearfield acoustical holography," J. Acoust. Soc. Am. **114**, 1322–1333 (2003).
[10] R. Steiner and J. Hald, "Near-field acoustical holography without the errors and limitations caused by the use of spatial DFT," Sixth International Congress on Sound and Vibration, Copenhagen, Denmark, 5–8 July (1999), pp. 843–850.
[11] J. Hald, "Planar near-field acoustical holography with arrays smaller than the sound source," 17th International Congress on Acoustics, Rome, Italy, 2–7 September (2001), Vol. **I**, Pt. A.
[12] M. Lee and J. S. Bolton, "Patch near-field acoustical holography in cylindrical geometry," J. Acoust. Soc. Am. **118**, 3721–3732 (2005).
[13] M. Lee and J. S. Bolton, "A one-step patch near-field acoustical holography procedure," J. Acoust. Soc. Am. **122**, 1662–1670 (2007).
[14] M. Lee and J. S. Bolton, "Reconstruction of source distributions from sound pressures measured over discontinuous regions: Multipatch holography and interpolation," J. Acoust. Soc. Am. **121**, 2086–2096 (2007).
[15] Y. T. Cho, J. S. Bolton, and J. Hald, "Source visualization by using statistically optimized near-field acoustical holography in cylindrical coordinates," J. Acoust. Soc. Am. **118**, 2355–2364 (2005).
[16] F. Jacobsen and V. Jaud, "Statistically optimized near field acoustic holography using an array of pressure-velocity probes," J. Acoust. Soc. Am. **121**, 1550–1558 (2007).
[17] J. Gomes, F. Jacobsen, and M. Bach-Anderson, "Statistically optimised near field acoustic holography and the Helmholtz equation least squares method: A comparison," Eighth International Conference on Theoretical and Computational Acoustics, Heraklion, Greece, 2–6 July (2007).
[18] Z. Wang and S. F. Wu, "Helmholtz equation–least-squares method for reconstructing the acoustic pressure field," J. Acoust. Soc. Am. **102**, 2020–2032 (1997).
[19] J. R. F. Arruda, "Analysis of non-equally spaced data using a regressive discrete Fourier series," J. Sound Vib. **156**, 571–574 (1992).
[20] B.-K. Kim and J.-G. Ih, "Design of an optimal wave-vector filter for enhancing the resolution of reconstructed source field by near-field acoustical holography (NAH)," J. Acoust. Soc. Am. **107**, 3289–3297 (2000).
[21] E. G. Williams, "Regularization method for near-field acoustical holography," J. Acoust. Soc. Am. **110**, 1976–1988 (2001).
[22] A. Kirsch, *An Introduction to the Mathematical Theory of Inverse Problems* (Springer-Verlag, New York, 1996), Chap. 2.
[23] G. H. Golub and C. F. Van Loan, *Matrix Computations*, 3rd ed. (Johns Hopkins University Press, Baltimore, MD, 1996).
[24] C. H. Harrison and P. L. Nielsen, "Plane wave reflection coefficient from near field measurements," J. Acoust. Soc. Am. **116**, 1355–1361 (2004).